PARTICLE VELOCITY FLUCTUATION IN A SEDIMENTING AGGREGATE OF UNEQUAL SPHERES

Gustavo Coelho Abade
Universidade de Brasília, Departamento de Engenharia Mecânica
Campus Universitário Darcy Ribeiro, 71090-900, Brasília - DF, Brasil
gcabade@unb.br

Francisco Ricardo da Cunha
Universidade de Brasília, Departamento de Engenharia Mecânica
Campus Universitário Darcy Ribeiro, 71090-900, Brasília - DF, Brasil
frcunha@unb.br

Abstract. *This work concerns with a numerical investigation of particle velocity fluctuations in a blob undergoing gravity induced sedimentation at low Reynolds number. The simulations were performed by direct computation of the hydrodynamic interactions between a large collection of spherical particles. We focus our attention on both monodisperse and slightly polydisperse spherical aggregates comprised of inertialess particles whose radii have a Gaussian distribution about the mean. At vanishing particle Stokes number the dispersed particles undergo stochastic displacements arising from the random ambient field of the fluid velocity and not from direct solid-body collisions. As the sedimentation proceeds, a monodisperse blob persists as a cohesive entity with sporadic outward particle crossings of the blob boundary. A scaling argument for the rate at which the particles leak away from the aggregate was developed. When a sufficiently high degree of polydispersity is introduced the aggregate will behave differently from a monodisperse blob depending on the solid volume fraction. The observed fluctuating motion of the particles leads to the definition of a particle pressure associated with the particulate phase of the blob if it is regarded as an effective continuum. For polydisperse blobs, the tendency to a particle spreading induced by velocity fluctuations makes clear the effect of the particle pressure on resisting the formation of solid volume fraction inhomogeneities in suspension flows.*

Keywords. *sedimentation, velocity fluctuation, hydrodynamic interaction, numerical simulation*

1. Introduction

In recent years, considerable attention has been focused on modelling the behaviour of fluid-particle systems, and in particular the behaviour of velocity fluctuations in a system of spherical particles sedimenting through a Newtonian fluid. In this context, computer simulations offer a way to gain some understanding on the complex relation between the microstructure of a suspension (i. e. the spatial arrangement of particles and their size distribution) and its macroscopic behaviour.

A class of algorithms known as Stokesian dynamics developed by Brady and Bossis (1988) has been widely employed in both Monte Carlo and dynamic simulations of suspension flow. This approach provides valuable results for the bulk properties of interest, such as effective viscosities, sedimentation rates, among many others. The problem of calculating hydrodynamic interactions among a large collection of particles and following their motion individually to determine average properties of the suspension can be computationally intensive. In the present work, the numerical method used to investigate particle velocity fluctuations in a sedimenting suspension is based on the Stokesian Dynamics approach and accounts for the long-ranged hydrodynamic interactions calculated in a pairwise additive manner.

In the midst of a sedimenting suspension, regions of particle density higher than average are constantly being formed and destroyed. These regions, to which one refers as blobs, may be studied in isolation in order to identify separately the mechanisms involved in the desintegration or preservation of such groups of particles. In this context, Nitsche and Batchelor (1997) investigated the consequences of the randomness of the particle trajectories on the behaviour of a cloud of particles sedimenting in a Newtonian fluid. They have performed simple calculations considering only a monopole representation of the hydrodynamic interactions. They reported that a group of particles clumped together in a nearly spherical blob remain together for long times. Their analysis, however, could not provide any insight into possible effects due to polydispersity of the particles.

Numerical simulations of the sedimentation process have been restricted mostly to monodisperse suspensions (Koch, 1994; Ladd, 1993). In this class of suspension, hydrodynamic interactions are the only source of velocity variance. One may expect that in polydisperse suspensions differences in particle settling rate provide an additional mechanism to the particle velocity fluctuations. This argument has attracted our interest to the role played by the polydispersity on the stability of the blob motion. By the term stability one means the feature of an aggregate in preserving itself as a cohesive entity during the sedimentation process.

In this work we concentrate on the density dependence of the macroscopic properties of a particle agglomerate as well as the underlying mechanisms that give rise to the observed behaviour. Our phenomenological investigation is based on a Lagrangian description of both particle and blob motions. One of the aims of the performed calculations is also to

show qualitative effects of the polydispersity on the blob motion. Here, are considered those cases in which the Reynolds number is zero and the Péclet number is infinite. The present analysis is also based on the assumption that the inertia of all particles is negligible.

This paper is organized as follows. In Section 2 the problem is described and the governing physical parameters are discussed. In Section 3 one presents a brief description of the mathematical formulation. We will not go into the details of the formulation, since they are covered in some depth in earlier publications (Abade and Cunha; 2001; Cunha *et at.*, 2002). Sections 4 and 5 present a short description of some aspects involved in the numerical method. In Section 6 a scaling argument for the mean sedimentation velocity of an aggregate is developed. The numerical results for static and dynamical simulations are presented and discussed in Section 7. Section 8 contains conclusions.

2. Statement of the problem

The problem under consideration consists of an aggregate comprised of hydrodynamically interacting spheres sedimenting under the influence of gravity through a Newtonian fluid of viscosity μ and density ρ_f with low-Reynolds-number flow about each particle. By the term aggregate is meant a finite region containing a nearly spherical dispersion of particles, with the geometric centre located at $\bar{\boldsymbol{x}}$. We shall denote by $\mathbb{A}_R(\bar{\boldsymbol{x}}) = \{\boldsymbol{x} : |\boldsymbol{x} - \bar{\boldsymbol{x}}| < R$ the blob domain and by $\partial\mathbb{A}_R$ its imaginary boundary. The complementary to $\mathbb{A}_R(\bar{\boldsymbol{x}})$ with respect to the cell domain Ω, denoted by $\mathbb{A}_R^c(\bar{\boldsymbol{x}})$, is filled by clear fluid.

Attention is focused on monodisperse and polydisperse suspensions with equidensity particles of varyzing radius. In Figure 1 it is shown a schematic representation of a polydisperse blob surrounded by clear fluid, under the action of a uniform gravitational field of intensity g.

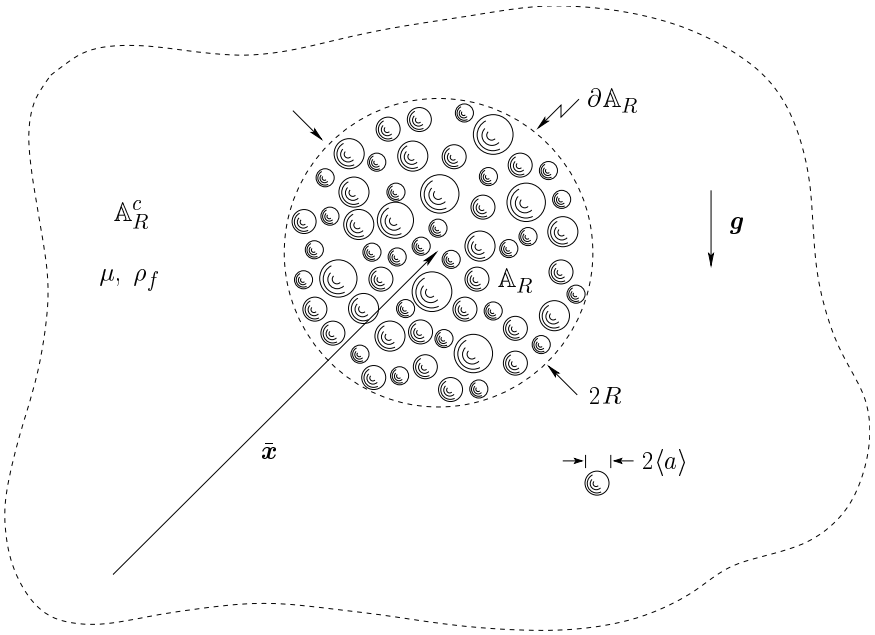

Figure 1: Scheme of a polydisperse blob suspended in a Newtonian fluid under the action of a uniform gravitational field of intensity g.

In order to better reproduce an actual suspension, it is considered polydispersions having a Gaussian particle-radius distribution with a controlled variance. The degree of polydispersity is measured by the relative spreading ν, defined by the ratio between the standard deviation in particle radii about the mean σ_a and the mean particle radius $\langle a\rangle$, as follows

$$\nu := \frac{\sigma_a}{\langle a\rangle} \tag{1}$$

For a monodisperse aggregate, the relative spreading ν vanishes.

Numerically, the Gaussian size distributions were generated by using the Box-Muller (1958) algorithm in the version of Marsaglia (1964) and Knuth (1969).

2.1. Physical parameters

The size of the particles is taken to be large enough so that the Brownian motion is no longer important in determining the suspension microstructure. We are only interested in the role played by the long ranged hydrodynamic interactions mediated by the suspending fluid. A measure of the relative importance of the random walk, due to the Brownian diffusion,

and the deterministic gravity induced motion is given by the Péclet number Pe, defined as

$$\mathrm{Pe} = \frac{U_0\langle a\rangle}{D_0} \tag{2}$$

where D_0 is the ordinary Stokes-Einstein diffusivity (Einstein, 1956), $U_0 = 2(\rho - \rho_f)\langle a\rangle^2 g/9\mu$ is the Stokes velocity and ρ denotes the particles density. The present investigation is restricted to the limiting case of $Pe \gg 1$.

As we have mentioned, the assumption of paramount importance is that the particle Reynolds number $\mathrm{Re} := \rho_f U_0\langle a\rangle/\mu$ is zero leading to drastic simplifications in the theoretical description of the suspension. The inertia of the suspending fluid is then negligible and the governing equation for the fluid motion becomes linear.

Another essential feature of the present study is that all particles are regarded to be inertialess. At this condition, the particle Stokes number, defined as

$$\mathrm{St} := \frac{mU_0}{6\pi\mu\langle a\rangle^2} \tag{3}$$

vanishes. At the low-Stokes-number regime, the particles respond instantaneously to hydrodynamic velocity disturbances in the interstitial fluid and fluid-mediated particle interactions play a dominant role in determining the particle velocity distribution.

The length quantities are made nondimensional using $\langle a\rangle$ as the characteristic length scale. Therefore, to each particle α of radius a_α is associated an aspect ratio $\lambda_\alpha := a_\alpha/\langle a\rangle$. Here, the subscripts α and β are employed exclusively for particle labelling. The Stokes hydrodynamic drag $6\pi\mu\langle a\rangle U_0$ is taken as the characteristic reference scale for force.

3. Mathematical formulation

The mathematical formulation of the problem is based on an Eulerian-Lagrangian description of the fluid-particle system. In such an approach the suspending fluid is treated as a continuum with no internal length scale and its motion is governed by the Stokes field equations obeying the appropriate conditions at the boundary of the system domain and at the surface of the particles. The discreteness of the particulate phase is fully taken into account and the motion of the particles is thus described individually. The particles motion is governed by the Newton's law and its description involves a set of ordinary differential equations for the $3N$ degrees of freedom of the particulate system. The equations are integrated numerically by using a fourth-order Runge-Kutta scheme.

The numerical system consists of a unit cell $\Omega = [0, d)\times[0, \ell)\times[0, h)$ containing an aggregate with N non-overlapping spherical particles in its interior. The simulation cell is replicated in a periodic manner filling the whole of space so that the blob microstructure in the unit cell is repeated in each direction.

Once specified the forces $\boldsymbol{F}_\alpha$ $(\alpha = 1, 2, \ldots, N)$ acting on the particles and assuming all particles to be torque-free, their translational velocities $\boldsymbol{U}_\alpha$ $(\alpha = 1, 2, \ldots, N)$ are determined by the mobility relation (Kim and Karrila, 1991)

$$\begin{pmatrix} \boldsymbol{U}_1 \\ \boldsymbol{U}_2 \\ \vdots \\ \boldsymbol{U}_N \end{pmatrix} = \begin{pmatrix} \boldsymbol{M}_{11} & \boldsymbol{M}_{12} & \cdots & \boldsymbol{M}_{1N} \\ \boldsymbol{M}_{21} & \boldsymbol{M}_{22} & \cdots & \boldsymbol{M}_{2N} \\ \vdots & \vdots & \ddots & \vdots \\ \boldsymbol{M}_{N1} & \boldsymbol{M}_{N2} & \cdots & \boldsymbol{M}_{NN} \end{pmatrix} \begin{pmatrix} \boldsymbol{F}_1 \\ \boldsymbol{F}_2 \\ \vdots \\ \boldsymbol{F}_N \end{pmatrix} \tag{4}$$

where the square matrix is the grand mobility matrix which contains the second-rank tensors $\boldsymbol{M}_{\alpha\beta}$ $(\alpha, \beta = 1, 2, \ldots, N)$. It should be noted that when carrying out the multiplication in the matrix equation (Eq. 4), the ordinary contraction between the tensors and vectors will be made.

The matrix $\boldsymbol{M}_{\alpha\alpha}$ is defined as the self-mobility associated with the αth particle and the matrix $\boldsymbol{M}_{\alpha\beta}$ is defined as the long-ranged two-sphere interaction mobility relative to the pair (α, β). For calculating the mobility tensors it was implemented the Ewald summation technique employing the method derived by Beenakker (1982). The numerical procedure to compute a far-field approximation to the grand mobility matrix has been described by Cunha *et al.* (2002), and we shall not repeat the detailed development.

Since the system is under the action of gravity and the particles are torque-free, the force $\boldsymbol{F}_\alpha$ acting on a particle α is given by

$$\boldsymbol{F}_\alpha = -\lambda_\alpha^3 \boldsymbol{e}_3 + \boldsymbol{f}^\alpha \tag{5}$$

The term $-\lambda_\alpha^3 \boldsymbol{e}_3$ is the net weight of the particle α and $\boldsymbol{f}^\alpha$ is a pairwise short-range repulsive interaction which mimics either lubrication or contact forces. These short-range forces are explained in more detail in the following section.

4. Sampling technique

The simulation of particulate systems involves an essential step which is the generation of particle distributions that accurately reflects the microstructure of a real system. The scheme to generate random particle configurations in the unit

cell depends strongly on the particle volume fraction. Since this study is restricted to dilute systems ($\phi < 0.27$), the generation procedure is quite simple and begins by placing sequentially the required number N of particles randomly within the cell domain Ω under the nonoverlap condition. The hard-sphere system is then subject to an equilibration process by employing the algorithm described in some detail in earlier publications (Abade and Cunha, 2001; Cunha *et al.*, 2002). As a result, the numerical procedure provides an ergodic ensemble comprised of samples consisting of equally probable nonoverlapping particle configurations. In Monte Carlo simulations, the generated particle arrangements constitutes the static configurations for which the transport properties of interest is calculated, and then averaged to obtain the mean values that describe the macroscopic behaviour of the system. In dynamic simulations the independent particle configurations constitute the initial condition of the suspension microstructure which evolves in time. In such class of simulation the configuration dependent properties of the system is calculated for thousands of time steps and ensemble averages are taken over several runs.

5. Pairwise interparticle forces

In the far-field representation of the hydrodynamic interactions considered here lubrication forces are not correctly accounted for and therefore we add an explicit short-range interparticle interaction to ensure that the particles will not overlap during the time evolution. In dynamic simulations, particle overlappings could produce large spurious effect on both particle and fluid velocity owing to the singularities of the far-field mobility functions.

The lubrication force is artificially modelled by the following expression (Cunha, 1995)

$$\boldsymbol{f}_{\ell}^{\alpha} = C_1 \eta_p \lambda_p^3 \exp\left[-\frac{\delta_{\alpha\beta}}{\lambda_p C_2}\right] \hat{\boldsymbol{r}}, \quad \text{for } 0 < \delta_{\alpha\beta} < \delta_0 \tag{6}$$

where C_1 and C_2 are arbitrary numerical parameters which represent, respectively, the intensity and the range of the repulsive force, $\delta_{\alpha\beta} = |\boldsymbol{x}_\beta - \boldsymbol{x}_\alpha| - (\lambda_s + \lambda_p)$ is the gap between the approaching particles and δ_0 is the interparticle gap for which the force $\boldsymbol{f}_{\ell}^{\alpha}$ is cut off.

Although the lubrication forces diverges when the particles come close providing a strong hydrodynamic resistance to particle contacts, it is considered in addition a restoring force $\boldsymbol{f}_{c}^{\alpha}$ due to eventual direct particle collisions arising from numerical inaccuracies. For simplicity it was employed a linear force-displacement relation for the interparticle contact in such a way that the normal elastic force is proportional to the virtual overlap $\varepsilon_{\alpha\beta} = -\delta_{\alpha\beta}$ (i. e. the relative displacement after initial contact) of the particles

$$\boldsymbol{f}_{c}^{\alpha} = -K \varepsilon_{\alpha\beta} \hat{\boldsymbol{r}}, \quad \text{for } \varepsilon_{\alpha\beta} > 0 \tag{7}$$

where K is the contact stiffness, assumed to be constant, whose value depends on the elastic and geometrical properties of the colliding particles.

It is worth noting that for suspensions of particles free of inertia, the introduction of contact forces between particles as we have made is just a numerical contrivance. Here, we are not interested in an accurate modeling of the interparticle contact since solid body collisions do not play a dominant role in determining the velocity distribution in a suspension of inertialess particles. Moreover, the macroscopic properties of the system were found to be insensitive to the force-displacement relation adopted for interactions of short-range nature.

6. Scaling arguments

If the aggregate is regarded as a continuous and a nearly spherical distribution of excess mass $4/3\pi R^3 \phi \rho$, a scaling argument for the mean sedimentation velocity $\langle U_a \rangle$ of the blob can be determined by balancing the Stokes drag with the net weight of the blob (the weight of the blob compensated for the Archimedian buoyancy force), as follows

$$6\pi\mu R \langle U_a \rangle \sim \frac{4}{3}\pi R^3 \phi (\rho - \rho_f) g \tag{8}$$

The velocity $\langle U_a \rangle$ is then taken to be

$$\langle U_a \rangle \sim \frac{2}{9\mu} \langle a \rangle^2 (\rho - \rho_f) g N \epsilon \tag{9}$$

where $\epsilon := \langle a \rangle / R$ and the solid volume fraction ϕ was approximated by $\phi \approx N\epsilon^3$.

In terms of the Stokes velocity,

$$\frac{\langle U_a \rangle}{U_0} \sim N\epsilon \quad \text{or} \quad \frac{\langle U_a \rangle}{U_0} \sim \phi \epsilon^{-2} \tag{10}$$

Considering that $\langle U_a \rangle / U_0$ approaches unity for the limiting case in which ϕ approaches 0

$$\frac{\langle U_a \rangle}{U_0} \sim 1 + S_a \phi_a \epsilon^{-2} \tag{11}$$

where S_a is an $O(1)$ sedimentation coefficient to be determined from the simulations.

7. Numerical results

7.1. Static simulations

In this section, results for the mean sedimentation velocity for monodisperse aggregates are presented in comparison with the scaling argument derived in the preceding section. The numerical results were obtained from Monte Carlo simulations for independent and random configurations of particles.

In Figure 2 the results for the mean settling velocity $\langle U_a \rangle$ as a function of the parameter $\phi\epsilon^{-2}$ are presented. The mean values and the statistical errors were evaluated over 30 random and independent static configurations. It is found that $\langle U_a \rangle$ increases monotonically with $\phi\epsilon^{-2}$ but deviates from the linear behaviour predicted by Eq. 11 at higher concentrations. In fact, the scaling argument is a leading order approximation and does not capture the effect of the hydrodynamic interactions. In the semidilute concentration range ($0 < \phi < 0.15$), the far-field approximation for the hydrodynamic interactions considered here provides results for the mean settling rate as a function of ϕ in good agreement with experimental correlations (Cunha *et al.*, 2002).

In the range of the parameter $\phi\epsilon^{-2}$ corresponding to the dilute regime, the numerical results for $\langle U_a \rangle / U_0$ yield good agreement with the relation given by Eq. 11 for a sedimentation coefficient $S_a = \frac{37}{20}$.

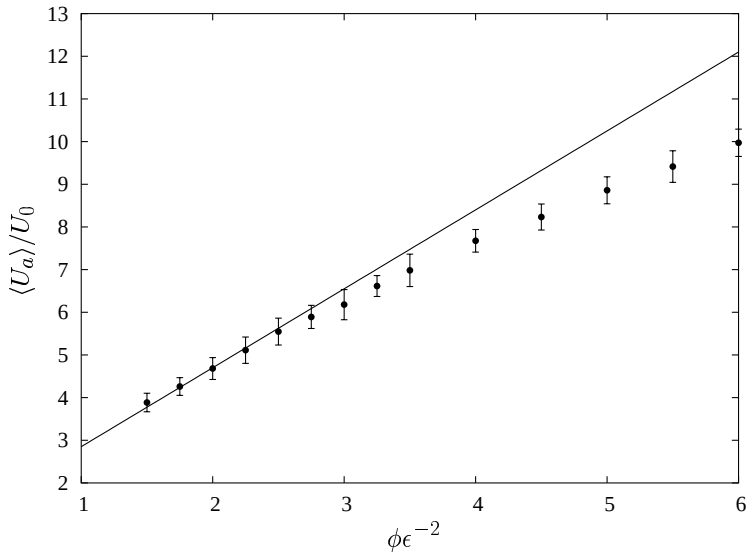

Figure 2: Mean settling velocity of a monodisperse aggregate as a function of the parameter $\phi\epsilon^{-2}$. The solid line is the linear fit $\langle U_a \rangle / U_0 = 1 + \frac{37}{20}\phi\epsilon^{-2} + O(\phi^2)$.

7.2. Dynamical simulations

In this section, results from dynamical simulations following the detailed motion of individual particles are presented. The simulations were carried out with aggregates comprising typically 300 particles. Different values for the solid volume fractions in the blob were then imposed only by varying its radius. The unit cell was taken to be large enough ($\ell/R \sim 10^3$) to minimize the long-range effects of the particle images replicated periodically throughout the space.

In dynamic simulations based on a mobility formulation, the sedimenting particles does not start from rest. Owing to the absence of particle inertia, at the initial stages of the time evolution the blob is already settling with terminal velocity which is much faster than the sedimentation velocity of the individual particles. If the motion is observed with respect to a frame of reference moving with the average sedimentation velocity, the particles initially placed at the periphery of the agglomerate are convected outward by the ascending flow. This causes a stretching of the blob which exhibits a temporary and significant deviation from the spherical shape. This initial regime seems to be intrinsic to the numerical procedure and also to the assumption that $St \ll 1$. We have reported that the transient sedimentation is as short as higher is the concentration of the blob. Such a transient regime occurring in a short period of time appears to be unrealistic, and therefore it will not be considered in the present analysis.

As the sedimentation proceeds, the blob motion evolves to a steady state regime when the aggregate recovers its roughly spherical shape. The aggregate remains cohesive while some particles escape from its interior very slowly. The quantitative analysis and the determination of the collective properties of the aggregate are restricted to the steady sedimentation.

Figure 3 shows the snapshots of a typical time evolution of a monodisperse aggregate. Figure 3a illustrates the initial regime, characterized by a strong particle flux across the blob boundary. The second regime is shown in Fig.

3b, and the long time coherence of the blob reported by Nitsche and Batchelor (1997) can be observed. Figure 3b also demonstrates that at the steady sedimentation the particles leak away from blob sporadically forming a wake of particles aligned vertically.

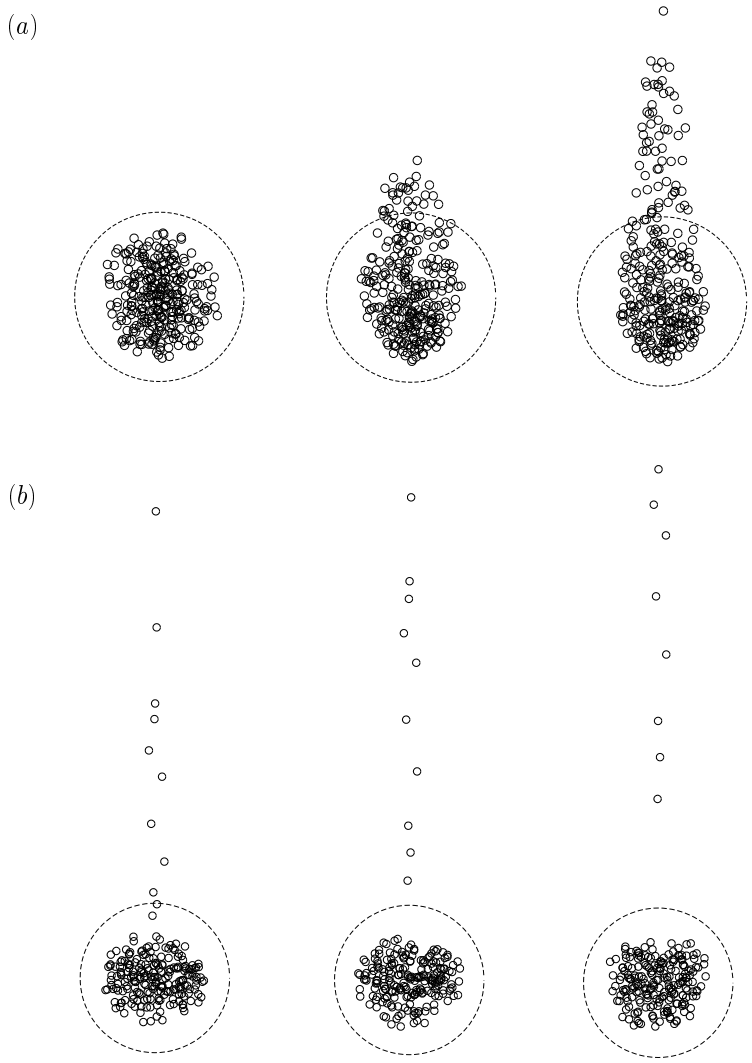

Figure 3: Typical time evolution of a sedimenting monodisperse aggregate with $\phi = 0.07$. The dashed circles represent the blob boundary. (a) Snapshots for the transient regime; (b) snapshots for the steady sedimentation.

7.3. Particle leakage from the blob

In order to determine the rate at which particles leak away from the blob, the number of particles leaving the aggregate was monitored. During the time evolution, a particle α with centre at $\boldsymbol{x}_\alpha$ is classified as belonging to the blob domain $\mathbb{A}_R(\bar{\boldsymbol{x}})$ if $|\boldsymbol{x}_\alpha - \bar{\boldsymbol{x}}| < \frac{5}{4}R$. This criterion, based on a cut off radius greater than R, ensures that small deviations of the blob geometry from the initial spherical shape will not mask the results for the particle leakage from the blob.

Before presenting the numerical results, an estimate of the rate at which the particles are shed may be derived by means of a simple physical argument. Such an argument is based on the idea that the particle flux across the blob boundary is induced by the velocity fluctuations V' about the mean.

The rate of particle crossings of a surface of area $\pi\epsilon^{-2}$ is given by

$$\frac{\mathrm{d}N}{\mathrm{d}t} \sim -nV'\pi\epsilon^{-2} \tag{12}$$

where n is the number density and V' denotes the velocity of the particles relative to the surface.

The magnitude of V', for the dilute limit, is given by (Cunha, 1995)

$$V' \sim \frac{\langle U_a \rangle}{\sqrt{N}} \tag{13}$$

where $\sqrt{N}$ is a typical fluctuation on N for a suspension of uniformly distributed particles. Invoking the Eq. 10, V' can be written as

$$V' \sim \epsilon\sqrt{N} \tag{14}$$

Substituting this result into Eq. 12 and using the definition of number density $n(= 3N/4\pi\epsilon^3)$, we obtain

$$\frac{\mathrm{d}N}{\mathrm{d}t} \sim -\frac{3}{4}N^{3/2}\epsilon^2 \tag{15}$$

Assuming that the blob radius remains constant with time, which seems to be reasonable for the steady regime, the integration of the Eq. 15 becomes straightforward. Carrying out the integration and after some algebraic manipulations, one obtains the following expression for the number of particles $\Delta N(t) := N_0 - N(t)$ that have leaked from the blob as a function of time t

$$\Delta N(t) \sim N_0 \left[1 - \frac{1}{(1+\kappa t)^2}\right] \tag{16}$$

where

$$\kappa \sim \frac{3}{8}\sqrt{N_0}\epsilon^2 \tag{17}$$

Figure 4 shows the number of particles that have leaked away from the blob as a function of the nondimensional time in comparison with the relation predicted by the Eq.16. The presented results are for monodisperse aggregates with $\phi = 0.03$ (Fig. 4a) and $\phi = 0.05$ (Fig. 4b). The numerical results plotted in Fig. 4 are in good agreement with the functional relation given by Eq. 16. To fit the curve to the computed points, we have adjusted the numerical constants involved in the Eqs. 16 and 17. Similar agreement has been verified for solid volume fractions in the range $0.07 < \phi < 0.15$.

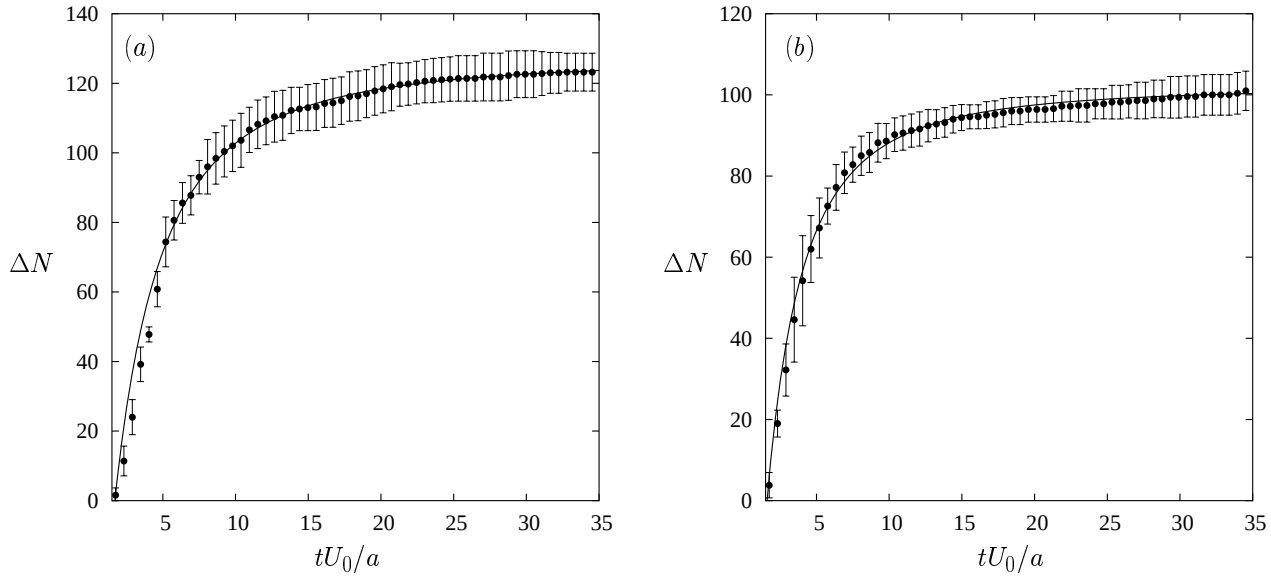

Figure 4: Numerical results for the number of particles that have shed from the blob as a function of the dimensionless time in comparison with the prediction given by Eq. 16. (a) $\phi = 0.03$; (b) $\phi = 0.05$.

Looking at the trajectories of the particles with respect to a frame of reference which moves with the average settling velocity of the blob, the ambient flow within the aggregate is very similar to the toroidal circulation observed in a sedimenting fluid drop (Batchelor, 1967). Owing to the hydrodynamic interactions, the particles exhibit stochastic motions superimposed to the deterministic gravity induced sedimentation. Figure 5a shows typical pathlines of some individual particles relative to the blob centre of mass located at $\bar{x}$. Figure 5b illustrates the trajectory of a particle which performed a circulatory motion in the interior of the blob and then reached its periphery being swept by the surrounding flow.

A close look at the pattern of particle trajectories presented in Fig. 5 allows us to speculate that the velocity fluctuations may depend on the size of the blob. This size dependence of the velocity fluctuations was verified from the present simulations for both monodisperse and polydisperse aggregates for different values of the parameter ν. In view of this, we cannot provide the concentration dependence for those effective properties arising from the particle velocity fluctuations in the microscale, such as particle pressure. Therefore, we will concentrate on a qualitative discussion concerning the effects of both solid volume fraction and polydispersity.

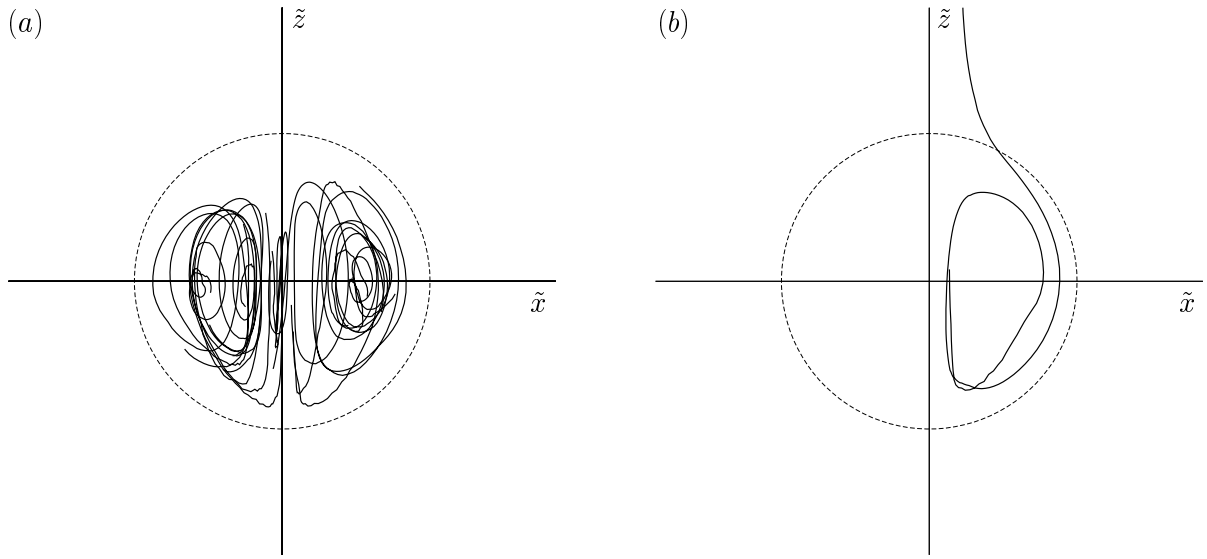

Figure 5: Typical pathlines of particles in the interior of the aggregate (a) and the trajectory of a particle which has leaked from the blob (b). The coordinates $\tilde{x}$ and $\tilde{z}$ are relative to the blob centre of mass $\bar{\boldsymbol{x}}$.

7.4. Effects of the polydispersity

In this section some effects of the polydispersity on the blob evolution are discussed qualitatively. In particular, we have focused on how polydispersity affects the particle velocity variance and the consequences on the global behaviour of a sedimenting blob.

As we have mentioned, differences in particle settling rates due to the polydispersity constitutes an alternative source of velocity fluctuations. Thus, one may expect that increasing the parameter ν, the velocity variance will increase as well as the rate of particle leakage.

Figure 6a shows the numerical results for ΔN as a function of time for an aggregate with $\phi = 0.09$ for three different values of the parameter ν. It can be seen that greater values of the rate of particle leakage are connected with greater values of the parameter ν. Such a result is in accordance with an intuitive argument that polydispersity intensifies the hydrodynamic interactions supplying energy to the particle velocity fluctuations. Thus, the lifetime of an aggregate with a polydispersity parameter sufficiently high tends to be smaller.

Figure 6b illustrates typical snapshots of sedimenting blobs ($\phi = 0.09$) with different values of the polydispersity parameter ν. It may be noticed from these pictures that for $\nu \leq 0.30$ there is no significant differences in the particle configurations at each instant of the time evolution. For this range of the parameter ν, the particles at the rear of the blob lie along a nearly vertical line. However, for $\nu = 0.4$, the blob performs observable deviations from its roughly spherical shape and the wake of particles emanating from the rear becomes thicker and unstable.

8. Conclusions

Numerical simulations of the microstructure of a sedimenting blob containing non-Brownian particles were performed in a scenario in which both particle and fluid inertia are negligible. From static simulations, results for the mean settling velocity of a monodisperse aggregate as a function of the parameter $\phi\epsilon^{-2}$ were obtained and found to be in agreement with scaling arguments at dilute conditions. Dynamic simulations of the blob flow showed that monodisperse and slightly polydisperse aggregates persists as cohesive entities with sporadic particle crossings of the blob boundary. The rate of particle shedding was determined for different solid volume fractions and compared with the prediction of simple scaling analysis.

At dilute conditions, we have reported that slightly polydisperse aggregates do not sediment differently from monodisperse ones. Aggregates with higher solid volume fractions seem to be more sensitive to the effects of polydispersity. When the degree of polydispersity is increased, the particles tend to spread out owing to their velocity variance. The intensification of particle velocity fluctuation decreases the time coherence of the blob. The observed fluctuating motion of the particles leads to the definition of a particle pressure associated with the particulate phase of the blob if it is regarded as an effective continuum. This tendency to a particle spreading makes clear the effect of the particle pressure on resisting the formation of solid volume fraction inhomogeneities in suspension flows.

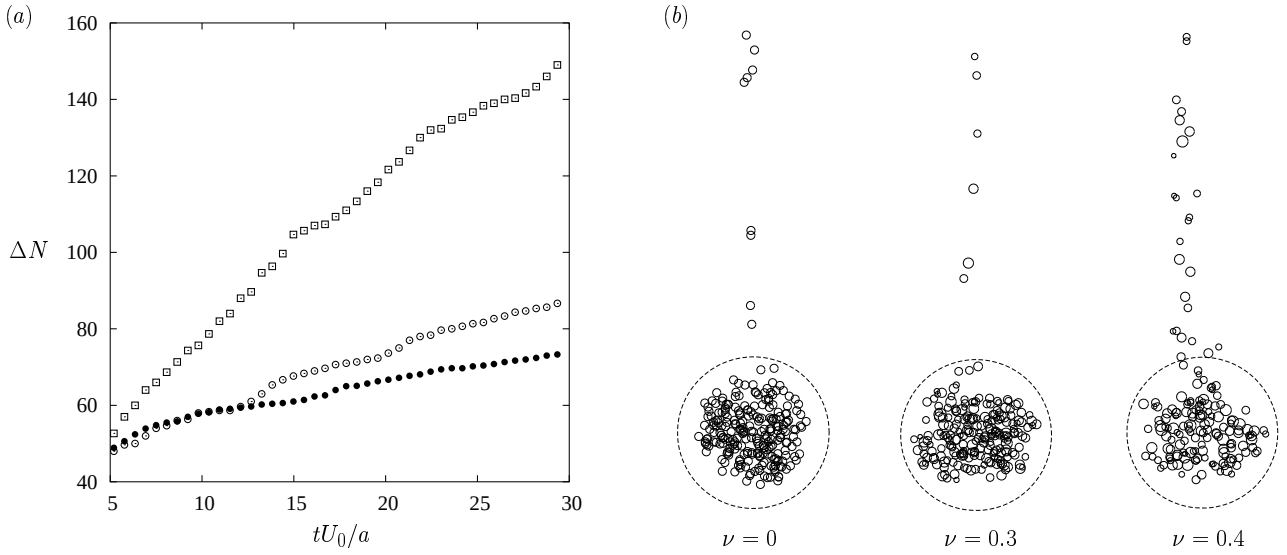

Figure 6: Illustration of the polydispersity effects on the time evolution of a blob with $\phi = 0.09$. (a) Numerical results for the number of particles that have shed from the blob as a function of the dimensionless time. •: $\nu = 0$; ○: $\nu = 0.30$; □: $\nu = 0.40$. (b) Representative snapshots at 25 $tU_0/\langle a \rangle$ for three different values of ν.

9. Acknowledgments

The authors greatfully acknowledge the CAPES and CNPq for the financial support.

References

Abade, G. C., Cunha, F. R., 2001. "Um Método Para Simulações Computacionais de Sistemas Particulados Randômicos Com Interação Hidrodinâmica", Anais do XVI Congresso Brasileiro de Engenharia Mecânica, Uberlândia, Minas Gerais.

Batchelor, G. K., 1967. "An Introduction to Fluid Dynamics", Cambridge University Press, Cambridge.

Beenakker, C. W. J., 1986. "Ewald Sum of the Rotne-Prager Tensor", J. Chem. Phys., Vol. 85,No. 3, pp. 1581-82.

Box, G. E. P., Muller, M., 1958. "A Note on the Generation of Random Normal Deviates," Ann. Math. Statist., Vol. 29, pp. 610-611.

Brady, J. F., Bossis, G., 1988. "Stokesian Dynamics", Ann. Rev. Fluid Mech., Vol. 6, pp. 111-57.

Cunha, F. R., 1995. "Hydrodynamic Dispersion in Suspensions", Doctoral dissertation, Department of Applied Mathematics and Theoretical Physics, University of Cambridge.

Cunha, F. R., Abade, G. C., Sousa, A. J., Hinch, E. J., 2002. "Modeling and Direct Simulation of Velocity Fluctuations and Particle-Velocity Correlations in Sedimentation", J. Fluids Eng. - ASME, Vol. 124, pp. 954-966.

Einstein, A., 1956. "Investigations on the Theory of the Brownian Movement", Dover, New York.

Kim, S., Karrila, S. J., 1991. "Microhydrodynamics: Principles and Selected Applications", Butterworth-Heinemann.

Knuth, D., 1969."The Art of Computer Programming," Volume 2, Addison-Wesley, Reading, Mass.

Koch, D. L., 1994. "Hydrodynamic Diffusion in a Suspension of Sedimenting Point Particles With Periodic Boundary Conditions," Phys. Fluids, Vol. 6, No. 9, pp. 2894-2900.

Ladd, A. J. C., 1993. "Dynamical Simulations of Sedimenting Spheres", Phys. Fluids A, Vol. 5, No. 2, pp. 299-310.

Marsaglia, G., MacLaren, M. D., Bray, T. A., 1964. "A Fast Procedure for Generating Normal Random Variables," Comm. ACM, Vol. 7, pp. 4-10.

Nitsche, J. M., Batchelor, G. K., 1997. "Break-up of a Falling Drop Containing Dispersed Particles", J. Fluid Mech., Vol. 340, pp. 161-175.